Volume 2
Number 6
November 2025
Pages 1191-1618

RSC Pharmaceutics

rsc.li/RSCPharma

eISSN 2976-8713

ROYAL SOCIETY OF CHEMISTRY

PAPER
Hlavačková *et al.*
Drug release from binary and ternary flexible dose combinations manufactured by drop-on-demand impregnation of mesoporous silica tablets

RSC Pharmaceutics

ROYAL SOCIETY OF CHEMISTRY

PAPER

View Article Online
View Journal | View Issue

Cite this: *RSC Pharm.*, 2025, **2**, 1447

Drug release from binary and ternary flexible dose combinations manufactured by drop-on-demand impregnation of mesoporous silica tablets

Zuzana Hlavačková,†[a] David Zůza,†[a] Erik Sonntag,[a] Jakub Petřík,[b] Ondřej Dammer[b] and František Štěpánek *[a]

Fixed-dose drug combinations (FDC) such as bi-layer tablets are known to improve treatment outcomes in polypharmacy patients thanks to better medication adherence achieved by reduced pill burden. However, the bulk manufacturing of FDCs is technically and economically viable only for such combinations where a sufficiently large patient cohort exists. The present work explores the "flexible dose combination" approach, which is based on the bulk manufacturing of placebo tablets containing mesoporous silica particles, and their subsequent impregnation by a combination of active pharmaceutical ingredients (API) at dosage strengths that can be adjusted to smaller patient cohorts or even individual patients. The present approach is based on volumetric dosing, which is generally faster and allows finer dosing steps than powder-based additive manufacturing methods. Specifically, this study investigates the potential of mesoporous silica-based tablets for the commonly prescribed triple combination of candesartan, hydrochlorothiazide, and amlodipine. Two grades of mesoporous silica were compared in terms of drug loading capacity and release kinetics for each API individually, and their binary and ternary combinations. Tablets containing Syloid 72FP showed superior performance in terms of drug release rates than tablets with custom-made mesoporous silica. The order in which the APIs were impregnated was found to be an important factor influencing drug release kinetics. The loading sequence candesartan–hydrochlorothiazide–amlodipine emerged as the best performing, enhancing amlodipine release and maintaining high release rates of hydrochlorothiazide and candesartan when compared to nanocomponent benchmarks. The findings prove that mesoporous placebo tablets loaded by the drop-on-demand method can effectively accommodate the triple drug combination, demonstrating their potential as a carrier system for flexible-dose formulations. At the same time, non-trivial API-specific dependence of drug release on the quantity and order of drug loading into the tablet was found, which must be considered when designing such formulations.

Received 12th March 2025,
Accepted 20th August 2025

DOI: 10.1039/d5pm00070j

rsc.li/RSCPharma

1 Introduction

Multi-drug formulations can be defined as pharmaceutical dosage forms that combine more than one active pharmaceutical ingredient (API) in a single drug product. The practicality of such formulations for patients stems from reducing the number of dosage units they must swallow. Reduced pill burden and consistent dosing often positively translates into improved medication adherence and superior treatment outcomes compared to the co-prescription of an equivalent combination of mono-component drug products.[1,2] The complexity of the medication regime is one of the most often cited reasons for medication non-adherence, which rises with the number of different medicines the patient must take. While adherence in patients taking only one medication is reported to be over 80%, this value decreases to about 50% in the case of four medications.[3] The combination of multiple active components is a common practice for ointments prepared individually in the pharmacy,[4] *e.g.* for antibiotics and corticosteroids. For mass-produced medicines, multi-drug tablets represent the most common form. These so-called Fixed Dose Combinations (FDCs) typically combine two or three APIs at a few dosage strength combinations chosen to cover a sufficiently large patient cohort for mass production and distribution to be worthwhile.[5] Between 2013 and 2018, almost 100 multi-drug formulations were approved by the regulatory authorities FDA (US Food and Drugs Administration) and EMA (European Medicines Agency).[6] Most of them focus on HIV,

[a]*Department of Chemical Engineering, University of Chemistry and Technology, Prague, Technická 3, Praha 166 28, Czech Republic.*
E-mail: Frantisek.Stepanek@vscht.cz; Tel: +420 220 443 236
[b]*Zentiva, k.s., U Kabelovny 130, 102 00 Praha 10, Czech Republic*
†Authors contributed equally.

respiratory diseases, diabetes, cardiovascular diseases, and hepatitis C.[7]

Depending on the physico-chemical compatibility of the APIs, FDC tablets can be manufactured either by the direct compression of powder blends containing multiple APIs, by individually granulating each API before tabletting to achieve their physical separation at the particle level, or by forming multi-layer tablets to achieve physical separation at the tablet level.[8–11] The physical separation of APIs in the formulation eliminates interactions that could cause API degradation, tablet hardening or other undesired phenomena that can occur during storage.[12] An inherent limitation of FDCs is that if the corresponding mono-component drug products are prescribed at multiple strengths, and two or three such APIs are to be combined into a single FDC drug product, the number of possible combinations raises in a geometric series. It is neither economical nor practical to mass-produce all such combinations.[13] Consequently, not all patients who could potentially benefit from FDCs are served. For example, one of the most often prescribed triple combination in the cardiovascular therapeutic area is the combination of candesartan, amlodipine and hydrochlorothiazide. Considering all combinations of currently marketed strengths of the nanocomponent drugs would result in (4–8–16–32 mg) × (2.5–5–10 mg) × (12.5–25–50 mg) = 36 combinations. Moreover, prescription practices by physicians within the same therapeutic area may differ. For example, instead of candesartan, some physicians might prefer to prescribe telmisartan, valsartan or losartan. The number of possible drug combinations and substitutions then rises even further.

New technologies such as additive manufacturing enable the production of multi-drug formulations with personalised composition from a theoretically unlimited combination of APIs at dosage strengths that can be freely adjusted. Numerous examples of 3D printed tablets containing sub-domains with different APIs have been reported in the literature,[14–16] including "polypill" prototypes with up to six different APIs.[17] Computational techniques for the rational design of 3D printed tablets with specifically required drug release profiles have been developed as well.[18–20] Methods typically used for fabricating 3D printed tablets include fused deposition modelling from a polymer filament,[21] syringe extrusion from a gel or paste,[22] binder jetting into a powder bed[23] or selective laser sintering.[24] While 3D printed tablets produced by fused deposition modelling are mainly the domain of research prototypes due to speed limitations,[25] tablets based on binder jetting have reached commercial-scale production[26] since liquid droplet dispensing can be performed at much higher speeds than polymer melt extrusion. Although polypills produced by additive manufacturing methods can in principle achieve full personalisation of the tablet composition, their practical use can be limited by factors such as excessive tablet size, which is caused by the need to include large quantities of excipients to make the formulation manufacturable by additive methods. The scalability of conventional additive manufacturing methods in terms of speed and drug degradation are additional factors that may complicate the mass implementation of polypills with customizable composition.

The present work explores an alternative approach, which aims to combine the benefits of industry-standard mass production of pharmaceutical tablets in a high-speed rotary tablet press with the flexibility of composition and dose customisation offered by liquid jetting. A method based on drop-on-demand impregnation of APIs into porous placebo tablets containing mesoporous silica has been recently demonstrated.[27] This concept was inspired by the old practice of delivering unpleasantly tasting medicines or vaccines to children by impregnating them into a sugar cube, which acts both as a taste masking agent and as a calibrated dose delivery system. In this work, the porous matrix of the sugar cube is replaced by a tablet containing a high proportion of mesoporous silica particles. Thanks to a large specific pore volume, mesoporous silica particles[28] are capable of storing and releasing a range of different APIs[29] with the added benefit of providing faster drug release due to amorphization.[30–33] Several studies have already explored various ways of improving the bioavailability of APIs such as candesartan,[34,35] amlodipine,[36,37] and hydrochlorothiazide.[38–41] The precise volumetric dosing of API solutions into prefabricated placebo tablets made from mesoporous silica particles then enables the manufacturing of multi-drug formulations with fully customisable composition and dosage strength.[42–44]

The feasibility and basic principles of this method have been recently demonstrated using model compounds.[27] It was shown that the drop-on-demand method is precise enough to meet pharmacopoeia specifications on content uniformity, but also that repeated impregnation and drying cycles can result in complex concentration patterns within the tablet. The aim of the present work it to explore this manufacturing concept in the case of triple-drug combinations using real APIs, namely amlodipine, candesartan and hydrochlorothiazide, which are among the most frequently co-prescribed APIs according to published statistics.[45] Mesoporous silica tablets were impregnated by each API individually and by their binary and ternary combinations at different sequences to investigate whether the loading order of the APIs had any influence on their release profiles. This knowledge is essential for reproducible and robust manufacturing of such multi-drug formulations.

2 Materials and methods

2.1 Materials

Tetraethyl orthosilicate (TEOS, 98%, CAS 78-10-4), cetyl trimethyl ammonium bromide (CTAB, 99%, CAS 57-09-0), Tween 20 (CAS 9005-64-5) and ammonium hydroxide (35%, CAS 1336-21-6) were purchased from Sigma Aldrich. Methanol (p.a., 100%, CAS 67-56-1), chloroform (99.9%, amylene stabilized, CAS 67-66-3), acetonitrile (chromatography grade, CAS 75-05-8), sodium chloride (NaCl, 99.9%, CAS 7647-14-5) and dihydrogen potassium phosphate (H_2KPO_4, 99%, CAS 7778-77-0) were purchased from Penta chemicals. Syloid 72 FP (CAS 7631-86-9),

Avicel PH 101 (CAS 9004-34-6), lactose monohydrate (CAS 10039-26-6), sodium lauryl sulphate (CAS 151-21-3), croscarmellose sodium (CAS 74811-65-7), magnesium stearate (CAS 557-04-0), amlodipine besylate (AML, CAS 111470-99-6, Batch No. AL19060005, manufactured by Hetero drugs Ltd, CoA purity: 100.2%), candesartan cilexetil (CAN, CAS 145040-37-5, Batch No. 5258-13-119, manufactured by Zheijang Huahai Pharmaceutical Co.) and hydrochlorothiazide (HCTZ, CAS 58-93-5, Batch No. RHCTP70156, manufactured by Unichem Laboratories Ltd) were kindly provided by Zentiva, k.s.

2.2 Silica particles

The custom-made silica particles were synthesized as described in ref. 46. The basic hydrolysis of TEOS in a water/ethanol mixture was catalysed by NH_4OH with CTAB as a surfactant. The synthesised SiO_2 was then calcined and stored as a powder until further use. Particles produced by this recipe were spherical with a high specific surface (>1000 $m^2\ g^{-1}$).[46] All experiments were done also with Syloid 72 FP for comparison with authority-approved products. Syloid 72 FP is a commercially available SiO_2 with a significantly lower specific surface (340 $m^2\ g^{-1}$) than synthesized silica.[48] However, the specific surface of the silica does not have to be the decisive factor in real-life applications.

2.3 Placebo tablet preparation

The tablets were prepared as described previously.[27] The tablet composition was identical for both Syloid and custom-made silica: 35 wt% SiO_2, 40 wt% microcrystalline cellulose (Avicel PH 101), 22.5 wt% lactose monohydrate, 0.5 wt% sodium lauryl sulphate, 1 wt% croscarmellose sodium and 1 wt% magnesium stearate. All ingredients were thoughtfully mixed for complete homogenization of the physical mixture. This mixture was then tabletted by a single-station semi-automatic tablet press (Natoli NP-RD10A) at 6 kN using round, flat-top punches of 10 mm in diameter. The tablets had a weight of 200 mg and a thickness of 3 mm. They were manufactured in batches of 50. It was previously found[27] that such silica tablets had a disintegration time of <1 min irrespective of drug loading and they were unaffected by exposure to organic solvents. The tablet hardness was 88 ± 5 N.

2.4 Drop-on-demand impregnation

The placebo silica tablets were impregnated with precise doses of API using a solution of the API in a suitable solvent (25 mg mL^{-1} in methanol for HCTZ and AML, and 40 mg mL^{-1} in methanol : chloroform 3 : 1 (w : w) mixture for CAN). The drug loading process consisted of repeated impregnation-drying cycles depending on the required quantity of each API. The API solution was dosed by a computer-controlled syringe pump Nemesys S (Cetoni GmbH, Germany), equipped with a glass syringe connected to a polytetrafluorethylene (PTFE) capillary (0.8 mm i.d.) as described previously.[27] The volumetric dosing accuracy was previously found to be less than ±5% of the nominal dose. The end of the capillary was positioned directly above the centre of the tablet, which was placed under a box cover to prevent premature solvent evaporation. Before the first loading, the tablets were dried in an oven at 45 °C for 15 min to remove atmospheric moisture that is naturally adsorbed in the silica particles. Between one and eight impregnation-drying cycles were conducted with each tablet, depending on the desired final dose of the API. The impregnation flow rate was set to 25 μL min^{-1}; thus, the loading part of each cycle took 2 min to complete. The drying part of the cycle was done in the oven at 45 °C for 15 min. These drying conditions are based on a previous analysis;[27] they were found to be sufficient to prepare the tablet for the next impregnation step and to completely remove any residual solvent after the last impregnation step.

The tablets were loaded by each API at two doses, namely 4 mg and 32 mg for CAN, 2.5 mg and 10 mg for AML, and 12.5 mg and 20 mg for HCTZ. These quantities represent the lowest and the highest marketed dose with the exception HCTZ where the high dose was limited to 20 mg to keep the number of loading cycles under eight, which was determined as a limit in the previous research.[27] Based on the API concentrations in the solvents used for impregnation, 32 mg of CAN represents a cumulative impregnation volume of 0.8 mL (8 impregnation-drying cycles), 10 mg of AML represents 0.4 mL (4 impregnation-drying cycles), and 20 mg of HCTZ represents 0.8 mL (8 impregnation-drying cycles). Then, every possible double combination of these APIs was loaded, including permutations. Finally, the triple combinations CAN–HCTZ–AML, CAN–AML–HCTZ and HCTZ–AML–CAN loading were prepared to investigate possible effects of loading sequence on drug release. The drug loading combinations and sequences are summarised in Table 1. All compositions were prepared in triplicates.

2.5 Tablet dissolution

Tablet dissolution experiments were carried out in a USP II apparatus (paddles, 75 rpm), 900 mL PBS pH 6.8 enriched with 0.35% Tween 20, which corresponds to the FDA dissolution guidance for this triple combination of drugs.[47] Samples of 1 mL were withdrawn *via* 10 μm syringe filter at 2, 5, 10, 15, 20, 25, 30, 45, 50 and 60 minutes. All dissolution experiments were done in triplicates and the resulting data points are reported as mean ± standard deviation. A validated HPLC method for accurate quantification of HCTZ, AML, and CAN was kindly provided by Zentiva, k.s. The analysis was carried out on HPLC Agilent 1260 equipped with quat. pump (G1311B), autosampler (G1329B), column comp. (G1316A), DAD (G1315D) and XBridge® C8 column (250 mm × 4.6 mm; 5 μm). The autosampler temperature and the column temperature were set to 37 °C. The separation of HCTZ, AML, and CAN was achieved by gradient elution (Table 2). The run time for the analysis was 12 min. All analytes were monitored at 255 nm.

The mobile phase A was a mixture of aqueous buffer and acetonitrile 80 : 20 (v/v); mobile phase B was a mixture of aqueous buffer and acetonitrile 20 : 80 (v/v). The aqueous buffer was prepared by pipetting 1 mL of triethylamine into 1 L of distilled water. The pH of such solution was then adjusted

Table 1 Summary of all tablet samples prepared in the course of this work. The drug loading is given in mg per tablet. One placebo tablet had a weight of 200 mg and contained 35 wt% of silica (Section 2.3). The composition of additional tablets not included in main body of the article can be found in the SI as Table S1

Sample name	Silica type	CAN [mg]	AML [mg]	HCTZ [mg]	Loading sequence (no. cycles, volume per cycle)
CAN_4.0 custom	Custom	4.0	—	—	CAN only (1 × 0.1 mL)
CAN_4.0 Syloid	Syloid	4.0	—	—	CAN only (1 × 0.1 mL)
CAN_32 custom	Custom	32.0	—	—	CAN only (8 × 0.1 mL)
CAN_32 Syloid	Syloid	32.0	—	—	CAN only (8 × 0.1 mL)
AML_2.5 custom	Custom	—	2.5	—	AML only (1 × 0.1 mL)
AML_2.5 Syloid	Syloid	—	2.5	—	AML only (1 × 0.1 mL)
AML_10 custom	Custom	—	10	—	AML only (4 × 0.1 mL)
AML_10 Syloid	Syloid	—	10	—	AML only (4 × 0.1 mL)
HCTZ_12.5 custom	Custom	—	—	12.5	HCTZ only (5 × 0.1 mL)
HCTZ_12.5 Syloid	Syloid	—	—	12.5	HCTZ only (5 × 0.1 mL)
HCTZ_20 custom	Custom	—	—	20.0	HCTZ only (8 × 0.1 mL)
HCTZ_20 Syloid	Syloid	—	—	20.0	HCTZ only (8 × 0.1 mL)
CAN–AML	Syloid	4.0	2.5	—	1. CAN, 2. AML
AML–CAN	Syloid	4.0	2.5	—	1. AML, 2. CAN
CAN–HCTZ	Syloid	4.0	—	5.0	1. CAN, 2. HCTZ
HCTZ–CAN	Syloid	4.0	—	5.0	1. HCTZ, 2. CAN
AML–HCTZ	Syloid	—	2.5	5.0	1. AML, 2. HCTZ
HCTZ–AML	Syloid	—	2.5	5.0	1. HCTZ, 2. AML
CAN–HCTZ–AML	Syloid	4.0	2.5	5.0	1. CAN, 2. HCTZ, 3. AML
CAN–AML–HCTZ	Syloid	4.0	2.5	5.0	1. CAN, 2. AML, 3. HCTZ
HCTZ–AML–CAN	Syloid	4.0	2.5	5.0	1. HCTZ, 2. AML, 3. CAN

Table 2 Gradient elution settings for HPLC analysis

Time (min)	% *A*	% *B*	Flow (mL min^{-1})
1.00	80	20	1.300
9.00	10	90	1.300
9.50	90	10	1.300
12.00	90	10	1.300

to a value of 6 by adding 0.4 mL of phosphoric acid (85% aq. sol.). The acetonitrile used to prepare the mobile phase was HPLC gradient grade.

2.6 Crystallinity measurement

It is known that API loading to mesoporous silica can lead to drug amorphization, but there is an upper limit on the amorphization capacity for each API.[48] To determine the amorphization limit for the three specific APIs and their combinations used in this work, X-ray powder diffraction (XRPD) data were collected at room temperature with an X'Pert PRO-θ–θ powder diffractometer with parafocusing Bragg–Brentano geometry using CuKα radiation (λ = 1.5418 Å, U = 40 kV, I = 30 mA). Tablets were crushed before the measurement. Data were scanned with an ultrafast detector X'Celerator (or with a scintillator detector equipped with a secondary curved monochromator) over the angular range of 5–60° (2θ) with a step size of 0.017° (2θ) and a counting time of 20.32 s per step. Data evaluation was performed in the software package HighScore Plus 3.0e.

2.7 Stress test of prepared formulations

The freshly prepared tablet containing a triple combination of CAN–HCTZ–AML (Table 1) was stressed for three days in a drying oven (Memmert 400) with a set temperature of 60 °C and relative humidity (RH) of 75%. Afterwards, the tablet was dissolved in a mixture of acetonitrile and methanol in a ratio of 1 : 1 (v : v) and then analysed by UPLC (Agilent 1290 Infinity) to determine if any degradation might have occurred due to drug interactions after silica impregnation. It should be noted that unlike classical tablets where the shelf life is measured in years, tablets impregnated by individualised mixtures of APIs are meant for immediate consumption (*e.g.*, storage for tens of days), and so the main purpose of the stress tests was to check for possible short-term incompatibility rather than long-term storage stability.

3 Results and discussion

3.1 Effect of silica type on drug release from single-API tablets

The drug release from tablets impregnated with each API individually was investigated first, to establish a baseline for subsequent studies of binary and ternary drug combinations. Each API was loaded at two doses ("low" and "high" according to its typical prescription) into tablets containing each type of mesoporous silica particles (*i.e.*, custom made silica and Syloid 72 FP), as specified in Table 1. The resulting drug release profiles are summarised in Fig. 1 (individual magnified dissolution curves can be found in the Fig. S1–S6). These results reveal the existence of three different drug release scenarios with respect to API dose in the tablet. In the case of HCTZ, practically 100% (within the standard deviation) was released from the tablets regardless of the silica type or drug loading level. On the other hand, neither CAN nor AML have reached full dissolution within 60 min in any of the silica/dose

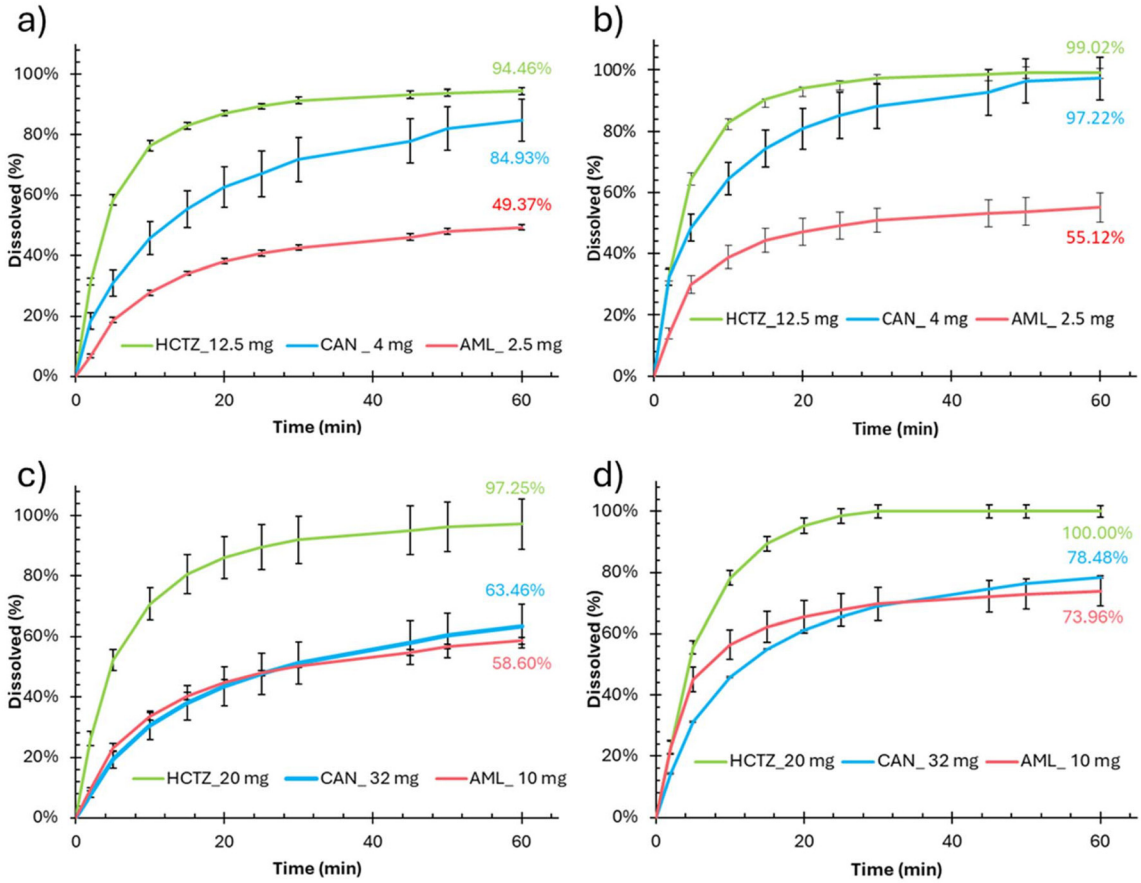

Fig. 1 Drug release profiles of individual APIs loaded to silica tablets. (a) Low dose in custom silica; (b) low dose in Syloid 72 FP; (c) high dose in custom silica; (d) high dose in Syloid 72 FP. The values by the curves denote percentage release of the dose after 60 min; the dose for each API is given in the legend.

combinations. Curiously, while the percentage release of CAN has decreased with increasing dose, the opposite was true for AML. Overall, tablets containing Syloid 72 FP perform better for all three APIs at both low and high drug loading than tablets made from the custom silica. Based on these results, only tablets containing Syloid 72 FP have been retained for subsequent studies of binary and ternary drug combinations.

The results shown in Fig. 1 can be interpreted by considering three factors: API solubility, silica amorphization capacity, and API-silica interaction (adsorption). The equilibrium solubility of HCTZ (2.24 mg mL^{-1} in H_2O at 25 °C) is much higher than that of CAN (0.00745 mg mL^{-1} in H_2O at 25 °C) or AML (0.0074 mg mL^{-1} in H_2O at 25 °C). HCTZ is also less hydrophobic (log *P* −0.16) than either CAN (log *P* 3.44) or AML (log *P* 2.22).[49] Hence, its complete dissolution after 60 min might not come as a surprise. For CAN in the low-dose tablets (Fig. 1a and b), complete release is probably just a matter of time as the release curves clearly maintain a positive slope at the 60 min mark and both appear to asymptotically converge towards 100% release. For the high dose CAN tablets (Fig. 1c and d), a reduction in the percentage release was observed (decrease from 85% to 63% for custom silica, and from 97% to 78% for Syloid). Nevertheless, it should be noted that out of the three APIs, CAN represents the highest absolute increase in the dose between the low and the high-dose scenarios (Table 1). Therefore, although the percentage release decreased, the absolute quantity of CAN dissolved from the tablets after 60 min still increased considerably: from 3.4 mg to 20.3 mg for custom silica, and from 3.9 mg to 25.1 mg for Syloid.

An opposite type of behaviour was seen for AML, where not only the absolute but also the percentage drug release increased for the increased dose (from 49% to 59% for custom silica, and from 55% to 74% for Syloid, which represents an absolute increase from 1.2 mg to 5.9 mg for custom silica and from 1.4 mg to 7.4 mg for Syloid, respectively). It is known from previous studies[48,50,51] that drug loading to mesoporous silica particles can improve the dissolution of poorly soluble APIs (BCS class II and IV) by amorphization. However, each silica-API combination has some upper limit (amorphization capacity) beyond which the dissolution rate enhancement is no longer effective. XRPD analysis of silica powder with all three APIs reveals that they remain amorphous even at the highest drug loading (Fig. 2). Therefore, crystallinity is unlikely to be the reason behind incomplete drug release.

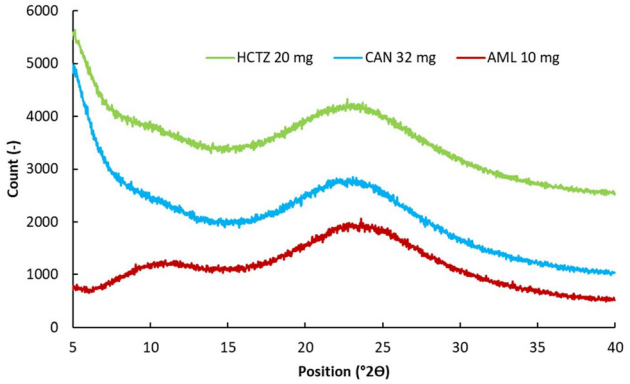

Fig. 2 XRPD patterns of Syloid 72 FP loaded with the highest doses of single APIs.

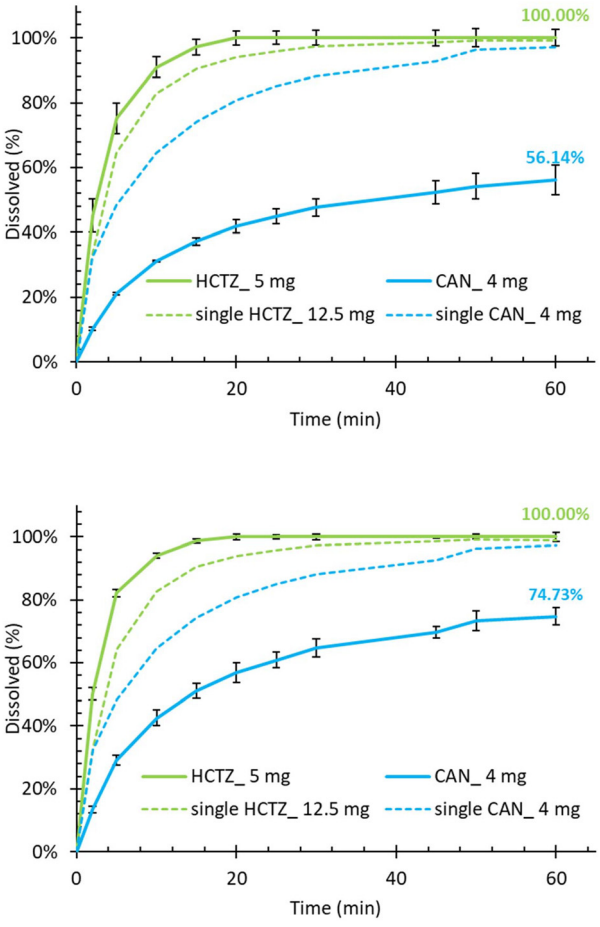

Fig. 3 Comparison of drug release from binary API combinations depending on the loading sequence. (a) HCTZ–CAN, (b) CAN–HCTZ (the first mentioned is the first loaded). For reference, the corresponding release curves from single-API tablets are shown as dotted lines.

However, it has been previously reported that apart from dissolution rate enhancement by amorphization, loading to mesoporous silica can sometimes lead to incomplete drug release due to too high affinity between the API and the silica surface (adsorption). A systematic study of this phenomenon on a sample of seven APIs and 4 different silica types was reported by Šoltys *et al.*[48] The underlying molecular interaction mechanisms were elaborated by Niederquell *et al.*[50] It can be hypothesised that a certain quantity of the API is adsorbed on the silica surface and the rest is free to be dissolved to the bulk of the dissolution medium. Due to the finite sorption capacity of the silica surface, increasing the absolute quantity of drug-loaded to the mesoporous silica carrier can result in an increase of both absolute and relative drug release, as was probably the case of AML here.

3.2 Binary API combinations in Syloid tablets

The effect of binary API combinations on drug release from porous tablets containing Syloid was investigated by comparing the dissolution curve of each API to its mono-component case, always for both permutations of the loading order. The dissolution curves are summarised in Fig. 3 (HCTZ with CAN), Fig. 4 (HCTZ with AML), and Fig. 5 (CAN with AML), respectively. Detailed dissolution profiles of binary API combinations from both types of silica carriers can be found in the SI (Fig. S7–S18). Very interesting and unexpected API interactions were found in these binary systems, indicating that not only the presence of another API, but also the order in which the two APIs were loaded to the porous carrier, and the solvent from which they were loaded, can influence the drug release of a co-loaded API both upwards and downwards compared to the single-API case.

In general, HCTZ was the least affected by the presence of another co-loaded API, whereas CAN was affected negatively, and AML positively. The release of CAN, which dissolved well from a single-API formulation, was significantly suppressed by the presence of a co-loaded API for both HCTZ (Fig. 3) and AML (Fig. 5). The suppression seemed to be slightly less severe when CAN was loaded as the first component (Fig. 3b and 5b) but occurred nonetheless. It is perhaps less surprising that the release of CAN was suppressed by the presence of AML, which dissolved poorly on its own and therefore it could potentially hinder or partially block the release of CAN from the silica mesopores. However, it was unexpected to see a similar effect for HCTZ, which dissolved very well on its own and so there was no *a priori* reason why it should hinder the dissolution of CAN as seen in Fig. 3.

On the other hand, the release of AML, which dissolved poorly from a single API formulation, was enhanced by the presence of another co-loaded API. This enhancement was more profound in the case of HCTZ (Fig. 4) than CAN (Fig. 5) but occurred in both cases. Interestingly, the dissolution rate enhancement was stronger when AML was loaded as the second component. A possible explanation could be that AML alone interacts strongly with the silica surface, but when another API is already present, it occupies the available adsorption sites, forcing AML to assume energetically less favourable sites. Ultimately, this promotes its release from the mesoporous silica matrix during dissolution as seen in Fig. 4.

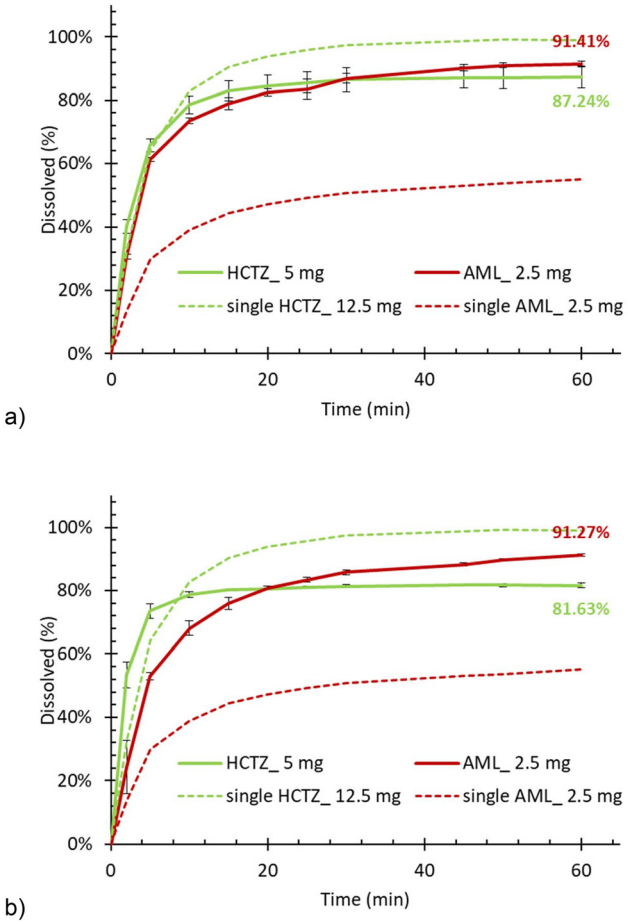

Fig. 4 Comparison of drug release from binary API combinations depending on the loading sequence. (a) HCTZ–AML, (b) AML–HCTZ (the first mentioned is the first loaded). For reference, the corresponding release curves from single-API tablets are shown as the dotted lines.

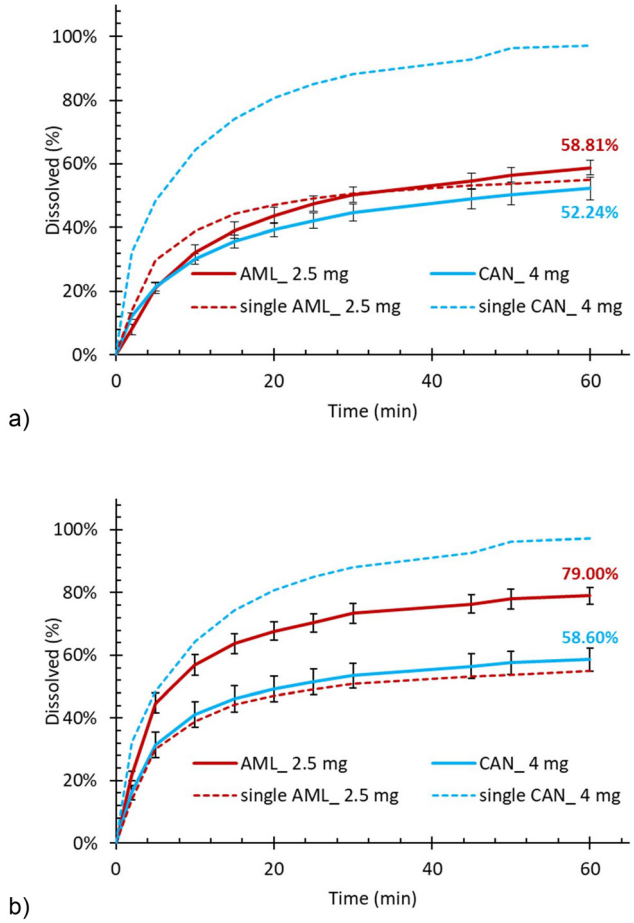

Fig. 5 Comparison of drug release from binary API combinations depending on the loading sequence. (a) AML–CAN, (b) CAN–AML (the first mentioned is the first loaded). For reference, the corresponding release curves from single-API tablets are shown as dotted lines.

It should be noted that drug–silica and drug–drug interaction at the pore level during the loading process also depends on the solvent from which the API was loaded. HCTZ and AML were both loaded from the same solvent (methanol), which means the when the second API was loaded, the first one could partially re-dissolve and both APIs could then re-deposit and find their thermodynamically most advantageous configuration in the porous silica matrix. Also, they mix with each other at the molecular level thanks to the common solvent. Consequently, the dissolution enhancement of AML when co-loaded with HCTZ was less sensitive to the order in which the APIs were loaded (Fig. 4). In contrast, CAN was loaded from a different solvent then AML. Thus, we can hypothesise that when CAN was loaded first, it could preferentially occupy the available sorption sites, leaving AML in a higher-energy state and ultimately promoting its release (Fig. 5b). When AML was loaded first, no such dissolution rate promotion occurred (Fig. 5a) as AML was not solubilised by the solvent from which CAN was loaded.

Several learnings can be taken from the results presented above. First, single-component drug release from a meso-porous silica matrix is a poor predictor of drug release for co-loaded APIs. Out of the three investigated APIs, only one (HCTZ) more-or-less retained its dissolution characteristics, while the dissolution of the other two was either suppressed (CAN) or enhanced (AML) by the presence of another co-loaded API. Furthermore, binary interactions of co-loaded APIs depend not only on the APIs themselves, but also on the order in which they were loaded to the porous carrier, and on the solvent from which they were loaded. To ensure the delivery of a defined dose of each API to the patient, these interactions must be considered and compensated *e.g.* by adjusting the quantity loaded to the carrier.

3.3 Ternary API combinations in Syloid tablets

The discussion in this section is focused on selected triple combinations; detailed dissolution profiles of all ternary API combinations from both types of silica carriers can be found in the SI (Fig. S20–S23). Based on the results from binary combinations presented above, in theory the best performing triple combination should be CAN–HCTZ–AML, as AML benefits

from co-loading as the second component after either CAN or HCTZ, while the dissolution of CAN was least affected when loaded before HCTZ. The loaded triple combination CAN–HCTZ–AML (Fig. 6) exhibited a decrease of HCTZ release in comparison to single loading by 13%; however, HCTZ performed better in the triple combination than in a double combination with AML alone. AML again benefited from co-loading with other APIs (5% increase); however, this effect was not as strong as in the double combination loading. CAN also behaves as expected, when its performance decreases by a significant amount as in previous double loadings (Fig. 6).

To explore the potential effect of the loading order on drug release from ternary combinations, the percentage release of each API after 60 min was compared with the theoretically loaded amount and with release obtained from a single-API tablet. This comparison is shown in Fig. 7 for three out of the six theoretically possible permutations, namely CAN–HCTZ–AML, CAN–AML–HCTZ, and HCTZ–AML–CAN. Analogous data for tablets made with custom silica can be found in the Fig. S20 and S21. As shown in Fig. 7 supposedly the best combination (CAN–HCTZ–AML) is indeed the best performer. As the only triple combination, it manifests an increase in AML dissolution, and the decreases for both HCTZ and CAN are smaller in comparison with other triple combinations. The switch between AML and HCTZ (CAN–AML–HCTZ) followed a similar trend as in the double combinations, as the release of both APIs decreased significantly. The ternary combination HCTZ–AML–CAN resulted in a lower overall drug release in comparison to the optimal and suboptimal combinations, as could be expected based on the binary systems (HCTZ–AML and AML–CAN). In general, it can be stated that while major shifts were observed when moving from single-API to double combinations, no similar surprises were found when moving from binary to ternary combinations as the shifts in this case occurred in the expected direction.

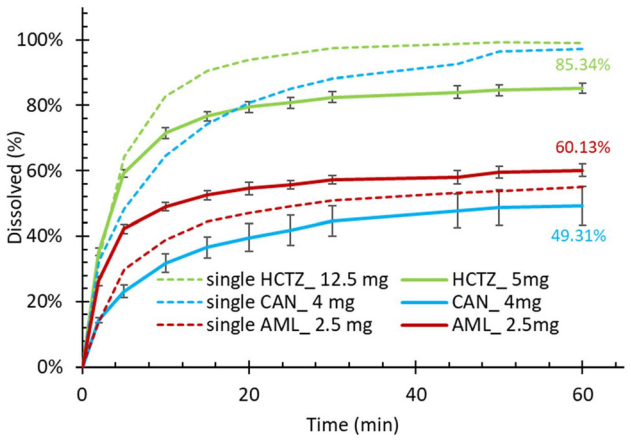

Fig. 6 The dissolution of triple combination CAN–HCTZ–AML from a Syloid tablet. The values by the curves denote the percentage release of the dose after 60 min; the absolute dose for each API is given in the legend. Full lines denote release from a triple combination tablet, dashed lines denote release from a single-API tablet.

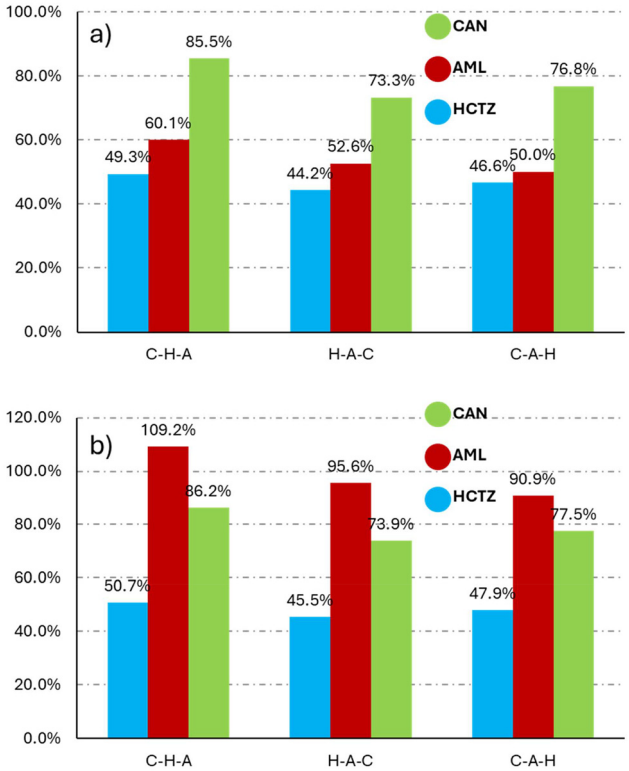

Fig. 7 The dissolved quantity of tested APIs after 60 min from triple combinations in Syloid tablets, expressed as percentage of the loaded quantity (a), and as percentage of release obtained during single-API loading (b). Note that in case (b) the values can exceed 100%.

3.4 Drug interaction scenarios

The results presented above raise a question of what the cause of reduced drug release, observed for co-loaded APIs, might be. The first possibility might be reduced solubility in the dissolution media. The original dissolution conditions were chosen to represent sink conditions for each API individually (*cf.* Section 2.5) but in theory, the APIs could decrease the solubility of each other when dissolved in combination. To test this hypothesis, the APIs were loaded to silica individually by the evaporation loading according to Šoltys *et al.*[48,52] The drug release from the powder was then observed for each API in a separate dissolution vessel and for all three powders in one common vessel. No decrease was observed in the fraction dissolved after 60 min from individual dissolution and from co-dissolution experiments. The full dissolution curves are provided in the SI (Fig. S19).

The second cause might be partial crystallinity of the samples, especially when all three APIs are loaded at the same time. It has been shown previously[27] that repeated loading cycles can increase crystallinity. To test this hypothesis, XRPD was used to compare empty and triple loaded tablets. As shown in Fig. 8, all crystalline bands in the tablets belong to lactose.

The third possible explanation could be degradation of the APIs. The freshly prepared tablet of CAN–HCTZ–AML was tested for impurities caused by drop-on-demand loading

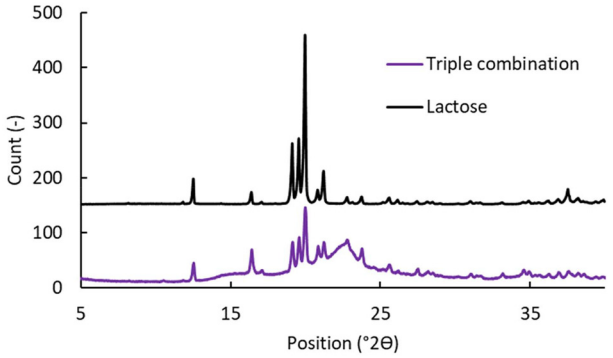

Fig. 8 The XRPD of ground triple combination tablet (purple) compared to lactose (black).

preparation. The results came out with a sum of impurities of 1.11% for AML, 2.45% for HCTZ and 9.43% for CAN. The results, while worthy further attention, cannot explain the more than 50% reduction of drug release observed for HCTZ and more than 20–25% reduction observed for CAN in some cases (Fig. 7b). Hence, the most likely explanation of reduced drug release from triple-API tablets compared to single-API ones appears to be synergistic co-adsorption, which might result in a stronger interaction between the co-loaded APIs and the silica carrier.

Without any ambition to provide a definite answer, let us postulate three hypotheses on the co-existence of multiple APIs within the mesoporous silica carrier: (i) the pore segregation hypothesis, (ii) the pore blocking hypothesis, and (iii) the pore mixing hypothesis. The pore segregation hypothesis (Fig. 9a) is based on the idea that each API preferentially occupies only specific pores. In this case, the APIs should theoretically not influence each other during dissolution. The pore blocking hypothesis (Fig. 9b) assumes that each API can occupy any pore if there is space for it, but the APIs do not mix at the molecular level. When multiple APIs are loaded onto the silica, the APIs could overlay each other and either restrict or promote each other's dissolution depending on their individual dissolution kinetics, affinity towards the silica surface, the order in which they were loaded and the relative quantity of each API. Finally, the pore mixing hypothesis assumes that each API can occupy any pore just like in the pore blocking hypothesis, but instead of forming segregated layers, the APIs can mix at the molecular level. The pore mixing hypothesis would mean that the APIs might strongly interact with each other and influence dissolution in a similar way as is known from co-crystals or co-amorphous systems. Based on the dissolution data presented above, the pore blocking hypothesis appears to be the most likely, but a certain contribution of the pore mixing hypothesis cannot be completely ruled. Certainly, this phenomenon deserves further research.

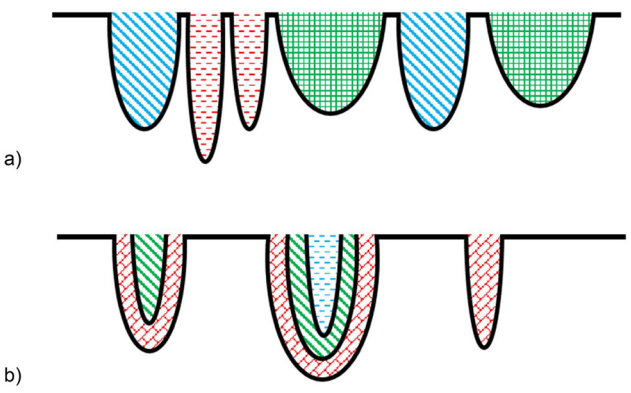

Fig. 9 Schematic representation of hypothetical distribution of multiple APIs within the pores of a mesoporous silica carrier, corresponding to (a) the pore segregation hypothesis, and (b) the pore blocking hypothesis. Different textures represent individual APIs.

4 Conclusions

The manufacturing of "flexible dose combination" tablets containing up to three different APIs with adjustable drug load has been investigated. By impregnating porous placebo tablets by precisely metered volumes of API solutions using the drop-on-demand method followed by solvent evaporation, tablets with individual APIs and their binary and ternary combinations have been prepared. This approach potentially has the advantage of combining the speed of the rotary tablet press for preparing the placebo tablets with the speed and precision of liquid dispensing to achieve the so-called "mass customisation" manufacturing concept, *i.e.* the production of small customizable batches of drug products for specific patient groups or even individual patients. Placebo tablets investigated in this work contained mesoporous silica particles as the drug carrier, which provided a high drug loading capacity but also resulted in non-trivial relationship between the drug dose and the release pattern, especially in the binary and ternary drug combinations. The drug release patterns were found to depend on the order in which the individual APIs were impregnated into the tablet, suggesting drug interaction such as competitive adsorption or layering had occurred at the pore-scale level. These factors must be considered when combining multiple APIs into mesoporous drug carriers to achieve a predictable relationship between composition and drug release.

The "mass customisation" approach presented in the present work can offer several benefits to patients. Conventional therapeutics (fixed dose tablets) are typically available only at a few strengths, which may not suit all patients. For example, geriatric patients or patients with specific metabolism or gastric conditions that deviate from the population average may need finer titration of the therapeutic dose than what is possible with fixed dose tablets. Furthermore, by combining multiple drugs into a single tablet, it is possible to reduce the so called "pill burden", *i.e.* number of dosage forms the patients must swallow. This may be particularly beneficial to patients with swallowing difficulties, in which case their adherence to prescribed medication could be improved.

Author contributions

Zuzana Hlavačková: methodology, investigation, visualization, data curation, writing – original draft; David Zůza: methodology, investigation, formal analysis, writing – original draft; Erik Sonntag methodology, investigation, writing – original draft; Jakub Petřík: methodology, investigation, writing – original draft; Ondřej Dammer: methodology, investigation, supervision, writing – review and editing; František Štěpánek: conceptualization, methodology, supervision, funding acquisition, writing – review and editing.

Conflicts of interest

The authors declare no competing interests.

Data availability

The data supporting this article are available on Zenodo at https://doi.org/10.5281/zenodo.15387800.

The supplementary information contains dissolution curves for all investigated monocomponent, binary and ternary drug combinations. See DOI: https://doi.org/10.1039/d5pm00070j.

Acknowledgements

This work was supported by the New Technologies for Translational Research in Pharmaceutical Sciences (NETPHARM), project ID CZ.02.01.01/00/22_008/0004607, co-funded by the European Union. The authors would like to acknowledge support from The Pharmaceutical Applied Research Centre.

References

1 M. Janczura, S. Sip and J. Cielecka-Piontek, The Development of Innovative Dosage Forms of the Fixed-Dose Combination of Active Pharmaceutical Ingredients, *Pharmaceutics*, 2022, **14**(4), 834.
2 N. J. Wald and D. S. Wald, The polypill concept, *Postgrad. Med. J.*, 2010, **86**(1015), 257–260.
3 N. A. Chaudri, Adherence to Long-term Therapies Evidence for Action, *Ann. Saudi Med.*, 2004, **24**(3), 221–222.
4 J. Cordonnier, Letter of the guidance of pharmacy and medication based on magistral preparations of mechlorethamine-based ointments, *Ann. Dermatol. Syphiligr.*, 1985, **112**(3), 293–293.
5 P. J. Crowley, *et al.*, *Development Programs for Oral Fixed Dose Combination Products*, in *Specialised Pharmaceutical Formulation: The Science and Technology of Dosage Forms*, ed. G. D. Tovey, The Royal Society of Chemistry, 2022.
6 K. I. Kaitin and J. A. Dimasi, Pharmaceutical innovation in the 21st century: New drug approvals in the first decade, 2000–2009, *Clin. Pharmacol. Ther.*, 2011, **89**(2), 183–188.
7 C. H. Andrade, L. M. de Freitas and V. de Oliveira, Twenty-six years of HIV science: An overview of anti-HIV drugs metabolism, *Braz. J. Pharm. Sci.*, 2011, **47**(2), 209–230.
8 K. M. Tserkovnaya, *et al.*, Polypill as a Personalized Dosage Form: Production Technology (Review), *Pharm. Chem. J.*, 2023, **57**(1), 108–115.
9 T. Taupitz, J. B. Dressman and S. Klein, New formulation approaches to improve solubility and drug release from fixed dose combinations: Case examples pioglitazone/glimepiride and ezetimibe/simvastatin, *Eur. J. Pharm. Biopharm.*, 2013, **84**(1), 208–218.
10 G. P. Andrews, *et al.*, Fixed Dose Combination Formulations: Multilayered Platforms Designed for the Management of Cardiovascular Disease, *Mol. Pharm.*, 2019, **16**(5), 1827–1838.
11 D. Desai, *et al.*, Formulation design, challenges, and development considerations for fixed dose combination (FDC) of oral solid dosage forms, *Pharm. Dev. Technol.*, 2013, **18**(6), 1265–1276.
12 O. N. Kavanagh, *et al.*, Maximising success in multidrug formulation development: A review, *J. Controlled Release*, 2018, **283**, 1–19.
13 C. A. Wilkins, *et al.*, Fixed-Dose Combination Formulations in Solid Oral Drug Therapy: Advantages, Limitations, and Design Features, *Pharmaceutics*, 2024, **16**, 178.
14 P. Robles-Martinez, *et al.*, 3D Printing of a Multi-Layered Polypill Containing Six Drugs Using a Novel Stereolithographic Method, *Pharmaceutics*, 2019, **11**(6), 274.
15 S. A. Khaled, *et al.*, 3D printing of five-in-one dose combination polypill with defined immediate and sustained release profiles, *J. Controlled Release*, 2015, **217**, 308–314.
16 B. J. Anaya, *et al.*, Engineering of 3D printed personalized polypills for the treatment of the metabolic syndrome, *Int. J. Pharm.*, 2023, **642**, 123194.
17 A. Xue, *et al.*, A Bibliometric Analysis of 3D Printing in Personalized Medicine Research from 2012 to 2022, *Pharmaceuticals*, 2023, **16**(11), 1521.
18 M. Novák, *et al.*, Virtual Prototyping and Parametric Design of 3D-Printed Tablets Based on the Solution of Inverse Problem, *AAPS PharmSciTech*, 2018, **19**(8), 3414–3424.
19 M. Kalný, Z. Grof and F. Štěpánek, Microstructure based simulation of the disintegration and dissolution of immediate release pharmaceutical tablets, *Powder Technol.*, 2021, **377**, 257–268.
20 Z. Grof and F. Štěpánek, Artificial intelligence based design of 3D-printed tablets for personalised medicine, *Comput. Chem. Eng.*, 2021, **154**, 107492.
21 S. Cailleaux, *et al.*, Fused Deposition Modeling (FDM), the new asset for the production of tailored medicines, *J. Controlled Release*, 2021, **330**, 821–841.
22 I. Seoane-Viaño, *et al.*, 3D printed tacrolimus suppositories for the treatment of ulcerative colitis, *Asian J. Pharm. Sci.*, 2021, **16**(1), 110–119.

23 K. A. van den Heuvel, *et al.*, 3D-Powder-Bed-Printed Pharmaceutical Drug Product Tablets for Use in Clinical Studies, *Pharmaceutics*, 2022, **14**(11), 2320.
24 E. Tikhomirov, *et al.*, Selective laser sintering additive manufacturing of dosage forms: Effect of powder formulation and process parameters on the physical properties of printed tablets, *Int. J. Pharm.*, 2023, **635**, 122780.
25 S. Wang, *et al.*, A Review of 3D Printing Technology in Pharmaceutics, Technology and Applications, Now and Future, *Pharmaceutics*, 2023, **15**(2), 416.
26 J. Norman, *et al.*, A new chapter in pharmaceutical manufacturing: 3D-printed drug products, *Adv. Drug Delivery Rev.*, 2017, **108**, 39–50.
27 M. Šoltys, *et al.*, Manufacturing of Multi-drug Formulations with Customised Dose by Solvent Impregnation of Mesoporous Silica Tablets, *AAPS PharmSciTech*, 2019, **20**(1), 1–10.
28 C. A. McCarthy, *et al.*, Mesoporous silica formulation strategies for drug dissolution enhancement: a review, *Expert Opin. Drug Delivery*, 2016, **13**(1), 93–108.
29 A. H. Ibrahim, *et al.*, Formulation and optimization of drug-loaded mesoporous silica nanoparticle-based tablets to improve the dissolution rate of the poorly water-soluble drug silymarin, *Eur. J. Pharm. Sci.*, 2020, **142**, 105103.
30 M. Kozakiewicz-Latała, *et al.*, Hierarchical Macro-Mesoporous Silica Monolithic Tablets as a Novel Dose–Structure-Dependent Delivery System for the Release of Confined Dexketoprofen, *Mol. Pharm.*, 2023, **20**(1), 641–649.
31 A. Baumgartner and O. Planinšek, Application of commercially available mesoporous silica for drug dissolution enhancement in oral drug delivery, *Eur. J. Pharm. Sci.*, 2021, **167**, 106015.
32 A. L. Doadrio, *et al.*, Mesoporous silica nanoparticles as a new carrier methodology in the controlled release of the active components in a polypill, *Eur. J. Pharm. Sci.*, 2017, **97**, 1–8.
33 J. Vyas, *et al.*, Potential Applications and Additive Manufacturing Technology-Based Considerations of Mesoporous Silica: A Review, *AAPS PharmSciTech*, 2023, **25**(1), 6.
34 R. Verma and D. Kaushik, Design and optimization of candesartan loaded self-nanoemulsifying drug delivery system for improving its dissolution rate and pharmacodynamic potential, *Drug Delivery*, 2020, **27**(1), 756–771.
35 M. Khanfar, B. Al Taani and E. Mohammad, Enhancement of dissolution and stability of candesartan cilexetil–loaded silica polymers, *Int. J. Appl. Pharm.*, 2019, **11**(2), 64–70.
36 D.-J. Jang, *et al.*, Improvement of bioavailability and photostability of amlodipine using redispersible dry emulsion, *Eur. J. Pharm. Sci.*, 2006, **28**(5), 405–411.
37 D.-J. Jang, T. Sim and E. Oh, Formulation and optimization of spray-dried amlodipine solid dispersion for enhanced oral absorption, *Drug Dev. Ind. Pharm.*, 2013, **39**(7), 1133–1141.
38 E. Essa, *et al.*, Hot melt extrusion for enhanced dissolution and intestinal absorption of hydrochlorothiazide, *J. Drug Delivery Sci. Technol.*, 2023, **88**, 104895.
39 M. M. Abdelquader, E. A. Essa and G. M. El Maghraby, Inhibition of Co-Crystallization of Olmesartan Medoxomil and Hydrochlorothiazide for Enhanced Dissolution Rate in Their Fixed Dose Combination, *AAPS PharmSciTech*, 2018, **20**(1), 3.
40 S. A. El-Gizawy, *et al.*, Aerosil as a novel co-crystal co-former for improving the dissolution rate of hydrochlorothiazide, *Int. J. Pharm.*, 2015, **478**(2), 773–778.
41 M. Ruponen, H. Rusanen and R. Laitinen, Dissolution and Permeability Properties of Co-Amorphous Formulations of Hydrochlorothiazide, *J. Pharm. Sci.*, 2020, **109**(7), 2252–2261.
42 A. Budiman and D. L. Aulifa, Encapsulation of drug into mesoporous silica by solvent evaporation: A comparative study of drug characterization in mesoporous silica with various molecular weights, *Heliyon*, 2021, **7**(12), e08627.
43 K. Trzeciak, *et al.*, Mesoporous Silica Particles as Drug Delivery Systems—The State of the Art in Loading Methods and the Recent Progress in Analytical Techniques for Monitoring These Processes, *Pharmaceutics*, 2021, **13**(7), 950.
44 W.-J. Sun, A. Aburub and C. C. Sun, A mesoporous silica based platform to enable tablet formulations of low dose drugs by direct compression, *Int. J. Pharm.*, 2018, **539**(1), 184–189.
45 S. Takai, *et al.*, Candesartan and amlodipine combination therapy provides powerful vascular protection in stroke-prone spontaneously hypertensive rats, *Hypertens. Res.*, 2011, **34**(2), 245–252.
46 M. Šoltys, *et al.*, Evaluation of scale-up strategies for the batch synthesis of dense and hollow mesoporous silica microspheres, *Chem. Eng. J.*, 2018, **334**, 1135–1147.
47 FDA dissolution database. [12.08.2024]; Available from: https://www.accessdata.fda.gov/scripts/cder/dissolution/dsp_getallData.cfm.
48 M. Šoltys, *et al.*, Drug loading to mesoporous silica carriers by solvent evaporation: A comparative study of amorphization capacity and release kinetics, *Int. J. Pharm.*, 2021, **607**, 120982.
49 Virtual Computational Chemistry Laboratory. [12.08.2024]; Available from: https://vcclab.org/lab/alogps/.
50 A. Niederquell, B. Vraníková and M. Kuentz, Study of Disordered Mesoporous Silica Regarding Intrinsic Compound Affinity to the Carrier and Drug-Accessible Surface Area, *Mol. Pharm.*, 2023, **20**(12), 6301–6310.
51 M. V. Speybroeck, *et al.*, Ordered Mesoporous Silica Material SBA-15: A Broad-Spectrum Formulation Platform for Poorly Soluble Drugs, *J. Pharm. Sci.*, 2009, **98**(8), 2648–2658.
52 M. Šoltys, *et al.*, Effect of solvent selection on drug loading and amorphisation in mesoporous silica particles, *Int. J. Pharm.*, 2019, **555**, 19–27.